Improving Signal/Noise Resolution in Single-Molecule Experiments Using Molecular Constructs with Short Handles

N. Forns,[†] S. de Lorenzo,[¶] M. Manosas,[‡†] K. Hayashi,[§] J. M. Huguet,[†] and F. Ritort[†¶*]

[†]Departament de Física Fonamental, Facultat de Física, Universitat de Barcelona, Barcelona, Spain; [‡]Laboratoire de Physique Statistique, École Normale Supérieure, Unité Mixte de Recherche 8550 associée au Centre National de la Recherche Scientifique et aux Universités Paris VI et VII, Paris, France; [§]Institute of Scientific and Industrial Research, Osaka University, Mihogaoka, Ibaraki, Osaka, Japan; and [¶]CIBER de Bioingeniería, Biomateriales y Nanomedicina, Instituto de Sanidad Carlos III, Madrid, Spain

ABSTRACT We investigate unfolding/folding force kinetics in DNA hairpins exhibiting two and three states with newly designed short dsDNA handles (29 bp) using optical tweezers. We show how the higher stiffness of the molecular setup moderately enhances the signal/noise ratio (SNR) in hopping experiments as compared to conventional long-handled constructs ($\cong$700 bp). The shorter construct results in a signal of higher SNR and slower folding/unfolding kinetics, thereby facilitating the detection of otherwise fast structural transitions. A novel analysis, as far as we are aware, of the elastic properties of the molecular setup, based on high-bandwidth measurements of force fluctuations along the folded branch, reveals that the highest SNR that can be achieved with short handles is potentially limited by the marked reduction of the effective persistence length and stretch modulus of the short linker complex.

INTRODUCTION

In the last years, many efforts have been made to increase the resolution of different single-molecule micromanipulation techniques, such as atomic force microscopy, optical tweezers, and magnetic tweezers (1). In all micromanipulation techniques, the molecule under study is attached to a force probe through a molecular handle. Molecular handles are used as spacers that prevent nonspecific interactions between the force probe and the molecule under study. In optical tweezers experiments, the molecular setup consists of the molecule of interest flanked by two handles (generally double-stranded nucleic acids), one handle located at each side of the molecule, and the whole construct is tethered between two polystyrene beads. One bead is trapped in an optical well and is used as a force probe, whereas the other bead is held fixed at the tip of a micropipette (Fig. 1 *A*). Similar constructs are used in dual-trap setups (2).

Under applied force, a DNA or RNA hairpin can unravel in a process reminiscent of what happens when the temperature is increased or the denaturant concentration changed. When the force applied on the hairpin is high enough (typically in the range 10–20 pN), the weak forces (hydrogen bonds plus stacking interactions) that maintain the hairpin structure are disrupted, and the hairpin unfolds. Previous studies with optical tweezers have investigated the folding/unfolding reaction of RNA and DNA molecules in real time using hopping experiments (3–6). In these experiments, the molecule executes transitions between different states while the trap-pipette distance is kept stationary (the passive mode (PM)) or the force is maintained constant at a preset value with a feedback system (constant-force mode (CFM)). These experiments have provided accurate information about molecular folding free energies and kinetics. More recently, it has been shown how handles affect the spatial and temporal resolution of single-molecule measurements (2,7,8). In the experiments, dsDNA handles of 1–10 kb are typically used. An analysis of the influence of their length on the folding/unfolding kinetics (7,8) revealed that longer handles (less stiff) tend to give faster kinetics and lower signal/noise ratio (SNR). Current single-molecule methodologies aim to use handles as stiff as possible to increase the resolution of the measurements. Although several kinds of stiff polymers might be suitable as molecular handles (e.g., carbon nanotubes (9) or microtubules (10)), the case of very short and rigid double-stranded nucleic acid handles has never been studied in detail. Is it feasible to carry out single-molecule experiments in the range where handles are very short, just a few tens of basepairs? What are the advantages of using molecular constructs with very short handles compared to conventional ones with long handles?

In this work, we introduce a minimal construct made of very short (29-bp) double-stranded DNA (dsDNA) handles to investigate DNA folding/unfolding kinetics. Since the handles are very rigid (their contour length is five times shorter than the persistence length of dsDNA), they are expected to behave like rigid rods that fully transmit the forces to the DNA hairpin. The results presented here correspond to two DNA hairpins with different folding landscapes: 1), a hairpin that folds and unfolds in a cooperative two-state manner (the 2S hairpin), and 2), a hairpin that has a fast intermediate-state on-pathway (the 3S hairpin). We have carried out hopping experiments using a highly stable miniaturized optical tweezers (11), and we have determined the full set

Submitted July 22, 2010, and accepted for publication January 31, 2011.

*Correspondence: fritort@gmail.com

F. Ritort's present address is Departament de Física Fonamental, Facultat de Física, Universitat de Barcelona, Barcelona, Spain.

Editor: David P. Millar.

0006-3495/11/04/1765/10 $2.00

doi: 10.1016/j.bpj.2011.01.071

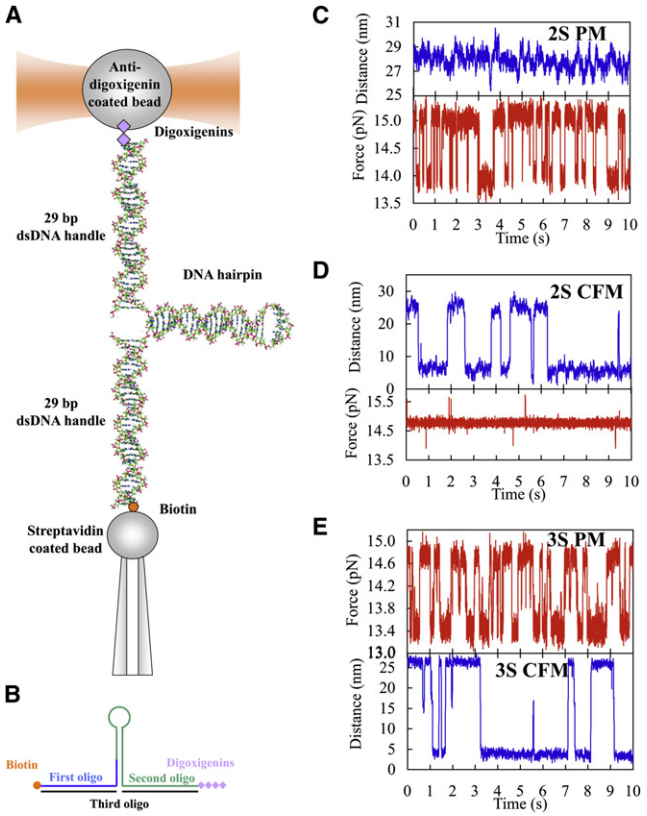

FIGURE 1 Experimental setup. (*A*) The molecular construct is attached between two beads, one held by the suction of a micropipette and the other captured in the optical trap. (*B*) Molecular construct with dsDNA short handles (29 bp/handle) made of three different oligonucleotides. (*C* and *D*) PM (*C*) and CFM (*D*) time-dependent trap-pipette relative distances (*upper*) and time-dependent force traces (*lower*) for the 2S hairpin with short handles. (*E*) PM time-dependent force trace (*upper*) and CFM time-dependent relative distances (*lower*) for the 3S hairpin with short handles.

of kinetic parameters describing the force folding kinetics and the free energies of formation of the different structures. In general, the results obtained with the new minimal construct are compatible with those obtained using the long-handled (500–800 bp) conventional construct. However, the new minimal construct increases the SNR only moderately and exhibits slower folding/unfolding kinetics, facilitating the detection of otherwise fast structural transitions. To evaluate and quantify the gain in SNR induced by the short handles, we have introduced, to our knowledge, a novel method based on the analysis of high-bandwidth noise force fluctuations at different stretching forces. This method provides a way to simultaneously measure the stiffness of the optical trap and the molecular system tethered between the beads.

MATERIALS AND METHODS

Synthesis of DNA hairpins with short handles

The designed DNA hairpins (see Section S1 in the Supporting Material) with short handles are synthesized using the hybridization of three different oligonucleotides (Fig. 1 *B*). This method of synthesizing the short handles is easier and faster to implement compared to the synthesis for long-handled hairpins. As it only requires labeling, hybridization, and ligation steps, one can avoid the multiple steps required for synthesis of longer double-stranded nucleic acids (e.g., polymerase chain reactions, digestion with restriction enzymes, phosphorylations, dephosphorylations, and DNA purifications). For the molecular setup and synthesis of the short- and long-handled constructs, see the procedure described in Section S2 and Fig. S2.

Force-dependent kinetic rates

We can determine the main parameters that characterize the free-energy landscape according to the Bell-Evans theory: $\Delta G_{SS'}$, B, $x^{\ddagger}_{SS}$, and $x^{\ddagger}_{S'S}$ (see Section S1 and Fig. S1 for a description of the free-energy landscape), by fitting the kinetic force-dependent rates to the expressions

$$k_{S\to S'} = k_m e^{\beta f x^{\ddagger}_{SS'}}, \tag{1a}$$

$$k_{S'\to S} = k_m e^{-\beta f x^{\ddagger}_{S'S}+\beta\Delta G_{SS'}}, \tag{1b}$$

where $\beta = 1/k_B T$, k_B is the Boltzmann constant, and T is the environmental temperature. S and S′ stand for the folded (F), unfolded (U), or intermediate (I) state. k_m corresponds to the unfolding rate at zero force. The term $\Delta G_{SS'}$ in Eq. 1b has been introduced to satisfy the detailed-balance condition. Coexistence rates, $k^C_{SS'}$, and coexistence forces, $f^C_{SS'}$, are defined by $k^C_{SS'} = k_{S\to S'}(f^C_{SS'}) = k_{S'\to S}(f^C_{SS'})$. To characterize the free-energy landscapes, we measured the different transition rates for the DNA hairpins using PM and CFM hopping experiments (12,7,8) (see Section S3).

In all cases, free-energy differences, molecular extensions, and coexistence forces also could be estimated from CFM and PM data by using the detailed-balance property or Van't Hoff equation,

$$\Delta G_{SS'}(f) = -k_B T \log(w_{S'}/w_S) = \Delta G_{SS'} - f x_{SS'}, \tag{2}$$

where $x_{SS'} = x^{\ddagger}_{SS'} + x^{\ddagger}_{S'S}$ and w_S and $w_{S'}$ are the statistical weights of states S and S′, respectively. In PM experiments, the weights in Eq. 2 are obtained from a Gaussian fit of the force distribution, whereas for the CFM experiments, the weights are measured from the time-dependent extension traces (see Section S4). The free energy of formation of both hairpins at zero force was obtained using the procedure described in Section S5. The procedure used to extract the mean lifetime of each state of the different hairpins from the time-dependent force traces (PM experiments) and extension traces (CFM experiments) is described in Section S4.

Measurement of SNR

The SNR is defined as the ratio between the jump in force in PM, or extension in CFM, in folding/unfolding transitions and the standard deviation of the signal. If s denotes a generic signal (force in PM experiments or trap position in CFM), then,

$$SNR_s = \Delta s/\sigma_s, \tag{3}$$

where Δs is the jump in the signal and σ_s is the standard deviation. To compare the new short-handled constructs with the standard long-handled constructs, we measured the SNR only in PM experiments (where s stands for the force). SNR measurements were done under PM conditions because in CFM experiments, the force feedback control operates at a frequency much lower than the corner frequency of the bead. For the determination of σ_f we collected high-frequency force data at 50 kHz using a data acquisition board (PXI-1033, National Instruments, Austin, TX). The chosen bandwidth of data collection is much higher than the corner frequency of the bead at all relevant forces (~2–3 kHz; see Section S6), a necessary condition for correct measurement of force fluctuations. Measurements of σ_f were taken for several molecules in a range of forces from 1 to 15 pN. Measurements

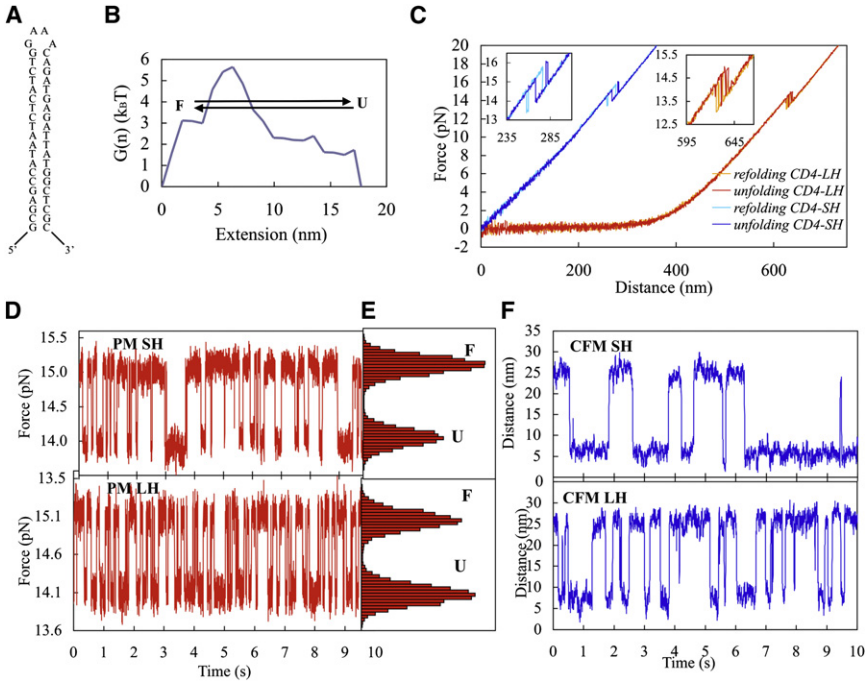

FIGURE 2 2S hairpin. (*A*) Sequence of the hairpin. (*B*) Free-energy landscape plotted as a function of the molecular extension (nm) at force $f = 14.6$ pN (at 25°C and 1 M NaCl). This was computed as described in Section S1. We also indicate the different transition rates (*arrows*). (*C*) FDC of pulling experiments with long and short handles. (*Insets*) Unfolding and refolding of the hairpin. (*D* and *E*) Force traces and distributions in the PM experiments for short- (*upper*) and long-handled (*lower*) constructs. (*F*) Time-dependent relative distances in the CFM experiments for the short- (*upper*) and long-handled (*lower*) constructs.

of Δf remained almost constant over the range of forces where hopping could be observed and were collected from hopping experiments.

RESULTS

Design of DNA hairpins with two and three states

We have designed to our knowledge a new construct (Fig. 1 *B*) that consists of a DNA hairpin inserted between two identical short dsDNA handles of 29 bp each (see Materials and Methods). These short handles are convenient to accurately follow the folding/unfolding transition, as they increase the total stiffness of the system, resulting in a better SNR (13,7,8). A conventional construct with 500- to 800-bp handles (see Section S2) has also been synthesized so that results obtained with both constructs can be compared. The molecular constructions are pulled by applying mechanical force to the ends of the DNA molecule under study (Fig. 1 *A*).

To test the new short-handled construct we investigated the force kinetics and thermodynamics of two different DNA hairpins, a two-state folder hairpin (2S) (Fig. 2 *A*) and a hairpin with an internal loop (3S) that presents an intermediate on-pathway (Fig. 3 *A*). By using the free-energy values from Mfold server at 25°C 1 M NaCl (14,15,8), the free-energy landscapes as a function of the molecular extension have been calculated for hairpins 2S and 3S at various forces (see Section S1). The predicted free-energy landscape of the 2S hairpin (Fig. 2 *B*) at the coexistence force of 14.6 pN shows two equal free-energy minima (corresponding to the folded (F) and unfolded (U) states) separated by a single free-energy barrier. The F and U states are separated by $\cong 18$ nm, which is equal to the extension of the released ssDNA when the hairpin unfolds at the coexistence force as measured in CFM experiments (18.2 ± 0.9 nm, averaged over eight molecules (see Figs. 1 *D* and 2 *F*)). The folding/unfolding reaction of the 2S hairpin can be schematically described by

$$\mathrm{F} \underset{k_{UF}}{\overset{k_{FU}}{\rightleftharpoons}} \mathrm{U},$$

where k_{FU} and k_{UF} denote the force-dependent unfolding and folding rates between states F and U as given by Eqs. 1a and 1b (see Materials and Methods).

The predicted free-energy landscape for the 3S molecule at the coexistence force between the folded and unfolded states (14.1 pN) shows the presence of an intermediate on-pathway generated by the entropy cost associated with the internal loop (Fig. 3 *B*). The sum of the distances between states F and I and states I and U at the coexistence force is 22.6 nm, consistent with the extension change measured during unfolding of the 3S hairpin in CFM, 22.0 ± 1.1 nm (averaged over nine molecules; see Figs. 1 *E* and 3 *F*). Four different transition rates describe the force kinetics in the 3S hairpin. These transition rates are described by the following scheme and are illustrated in Fig. 3 *B*:

$$\mathrm{F} \underset{k_{IF}}{\overset{k_{FI}}{\rightleftharpoons}} \mathrm{I} \underset{k_{UI}}{\overset{k_{IU}}{\rightleftharpoons}} \mathrm{U}$$

where k_{FI}, k_{UI}, k_{IU}, and k_{IF} stand for the force-dependent transition rates between states F, I, and U as given by Eqs. 1a and 1b (see Materials and Methods).

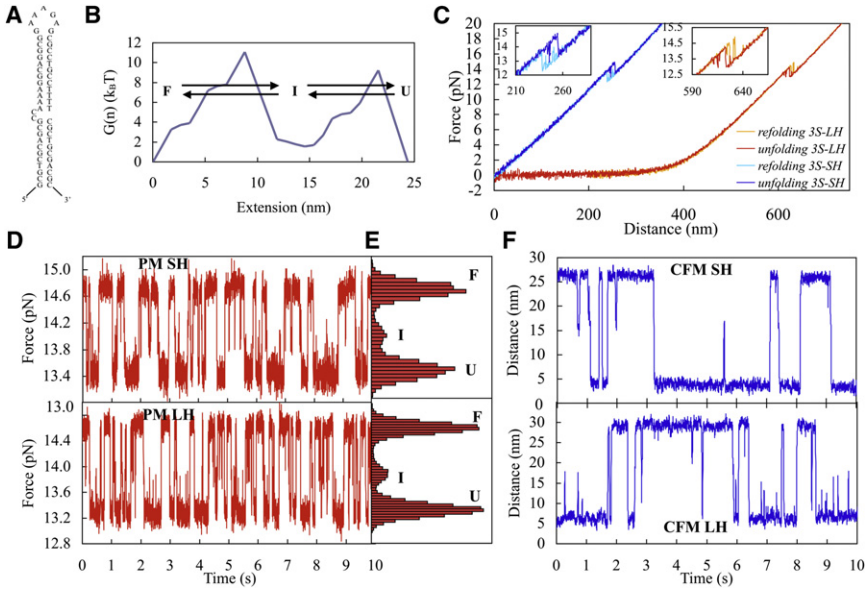

FIGURE 3 3S hairpin. (*A*) Sequence of the hairpin. (*B*) Free-energy landscape plotted as a function of the molecular extension (nm) at force $f = 14.1$ pN (at 25°C and 1 M NaCl). This was computed as described in Section S1. We also indicate the different transition rates (*arrows*). (*C*) FDC of pulling experiments with long and short handles. (*Insets*) Unfolding and refolding of the hairpin. (*D* and *E*) Force traces and their distribution in the PM experiments for the short- (*upper*) and long-handled constructs (*lower*). (*F*) Time-dependent relative distances in the CFM experiments for the short- (*upper*) and long-handled (*lower*) constructs.

Pulling experiments (see Section S3), in which the force is first increased to unfold the hairpin and then decreased to allow the hairpin to refold (3,16), were initially performed with the two different constructs (short and long handles) for both hairpins. The force-distance curves (FDCs), corresponding to the measured force as a function of the distance between the center of the trap and the tip of the micropipette recorded at a pulling speed of 26 nm/s, are shown in Figs. 2 *C* and 3 *C*. The first part of the FDC corresponds to the elastic response of the dsDNA handles, and it clearly differs between the two constructs. The FDCs corresponding to the short-handled construct show no curvature due to the high stiffness and shorter length of the handles. In contrast, the FDCs for the long-handled construct show a curvature consistent with the larger elastic compliance of a longer dsDNA molecule. As the hairpin unfolds, the bead in the optical trap relaxes and the tension decreases, generating a force jump in the FDC. The folding/unfolding transition for the 2S molecule is a two-state transition, whereas for the 3S molecule, an intermediate state with a very short lifetime can be detected. The force jump obtained during the unfolding transition is nearly the same for both constructs: 1.14 ± 0.06 pN and 1.56 ± 0.08 pN (averaged over 10 molecules) for the 2S and 3S hairpins (see Figs. 2 *C* and 3 *C*, *insets*). The force jump can be converted into the molecular extension difference between the folded and unfolded conformations by dividing it by the effective stiffness of the molecular setup (6). The latter is given by the slope of the FDC along the folded branch measured at the unzipping force. This gives the aforementioned 17.4 ± 0.9 nm and 23.5 ± 1.2 nm (averaged over 10 molecules) released distances for the 2S and 3S molecules, respectively, values that are in agreement with the free-energy landscape predictions (Figs. 2 *B* and 3 *B*). Although experiments with both constructs were performed at the same pulling speed, more folding/unfolding transitions along the FDC were observed with the long-handled construct, suggesting that the folding/unfolding kinetics is slowed down when using shorter handles.

Force-dependent kinetic rates measured in hopping experiments

To study in detail the force folding/unfolding kinetics for the two hairpins, we carried out PM and CFM hopping experiments (7,8,12) (see Figs. 1, *C–E*, and 2, *D* and *F*). The unfolding and folding processes were followed by recording force traces (PM experiments) or extension traces (CFM experiments) over time. Time traces typically span a few minutes at each condition. Since the DNA hairpin undergoes repeated cycles of folding and unfolding transitions under either mode, lifetimes in each state can be measured many times from one single experiment, making these hopping experiments useful for extracting kinetic parameters such as coexistence rates, $k^C_{SS'}$, and coexistence forces, $f^C_{SS'}$. S and S′ stand for the folded (F), unfolded (U), or intermediate (I) states. By applying the Bell-Evans theory, we can determine the main parameters that characterize the force-dependent kinetic rates (see Materials and Methods and Section S4). In all cases, free-energy differences, molecular extensions, and coexistence forces associated to the folding/unfolding transition could also be estimated from PM or CFM data using the detailed-balance condition of Eq. 2 (see Materials and Methods for details).

Results for the 2S hairpin

Typical traces in the PM and CFM for the 2S hairpin are shown in Fig. 1, *C* and *D* (for the short-handled construct) and in Fig. 2, *D* and *F* (for short- and long-handled

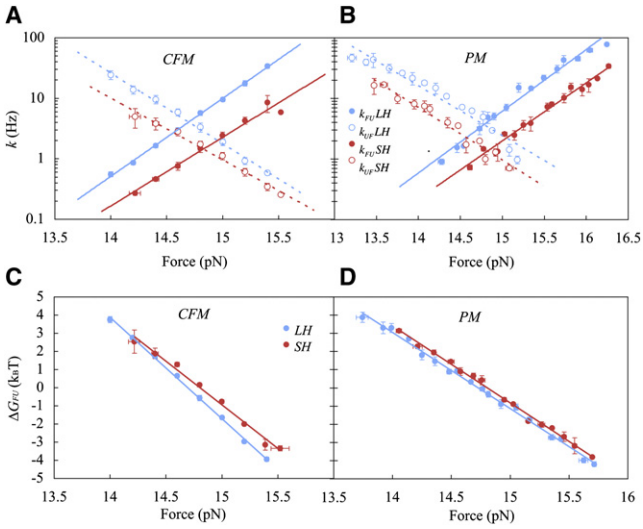

FIGURE 4 Results for the 2S hairpin with short handles (*red* or *dark gray*) and long handles (*blue* or *light gray*) (color online). (*A* and *B*) Plots of k as a function of force for CFM experiments (*A*) and PM experiments (*B*) and the linear fit (*lines*) for the log of the rates, where solid symbols and lines represent the unfolding rate (k_{FU}) and dotted symbols and lines the folding rate (k_{UF}). (*C* and *D*) Plots of the ΔG_{FU} versus force for CFM (*C*) and PM (*D*) experiments and their linear fit (*lines*). We show the mean values for each point and the standard error. Molecule statistics are presented in the note to Table 1.

constructs), and a frequency histogram for a force trace in the PM is shown in Fig. 2 *E*. The hopping traces obtained with the long- and short-handled constructs are very similar (Fig. 2, *D* and *F*). In particular, the differences in molecular extension between the folded and unfolded conformations extracted from the CFM experiments are equal for both constructs ($\cong$18 nm). On the other hand, the small difference measured for the force jump in the PM (1.07 $\pm$ 0.05 pN for long handles and 1.15 $\pm$ 0.06 pN for short handles, as obtained from averaging results over five molecules in both cases) is consistent with the lower effective stiffness of the long-handled construct (7,8) (see below). The main difference observed between experimental traces obtained with both constructs is the presence of a higher number of folding/unfolding transitions for long handles. Indeed, at all forces measured, the values obtained for kinetic rates are found to be larger with the long-handled construct for both PM and CFM (see below).

The results for the fitting parameters obtained by both methods, the Bell-Evans theory (Eqs. 1a and 1b) (Fig. 4, *A* and *B*) and detailed balance (Eq. 2) (Fig. 4, *C* and *D*), are shown in Table 1. For the PM case, the molecular extension obtained from both methods agrees well with that measured from the PM traces and the predicted value from the free-energy landscape (see Section S5). In contrast, the molecular extensions obtained from both methods in CFM experiments are larger (21–23 nm) than either the extension change directly measured from the CFM traces (~18 nm) or the predicted value (18 nm). The same effect is observed for the 3S hairpin (see next section). This artifact is a consequence of the finite operational frequency of the feedback control in CFM experiments (1 kHz) (Phillip Elms, University of California, Berkeley, personal communication, 2010).

As expected, the thermodynamic parameters are almost independent of the construct (results for short and long handles differ by <10%), but the kinetic parameters (such as the transition rates) change with the length of the handles, as previously reported (7,8). In particular, whereas the measured values of ΔG^0_{FU} in both constructs differ by <10% (Section S5 and Table S5), the coexistence rate measured with the long-handled construct (low stiffness) is around three to four times higher than that measured with the short-handled construct (high stiffness) (Table 1 and Fig. 4, *A* and *B*). Let us note in passing that, apart from the PM and CFM coexistence rates (k^C_{FU}), we can also measure the so-called apparent coexistence rate (k^C_{app}) in the PM experiments. These rates are the ones measured in PM but plotted as a function of the average force between the folded and unfolded states (see Section S7). It has been reported that k^C_{app} decreases with trap stiffness in DNA hopping experiments (2). This is in contrast to what happens with the coexistence rates, k^C_{FU}, measured throughout this study, which increase for a less stiff setup (e.g., longer handles). We have verified that whereas k^C_{app} decreases with trap stiffness, the k^C_{FU} increases (see Section S7, Table S7, and Fig. S7). This is in agreement with results from previous studies (2).

Results for the 3S hairpin

Hopping traces in the PM and CFM for the 3S hairpin (Figs. 1 *E* and 3, *D* and *F*) reveal the presence of a short-lived intermediate state (mean lifetime ~10 ms). By comparing the hopping traces for long and short handles, we confirmed the trends observed in the 2S hairpin. The force jump between folded and intermediate states is equal to 0.91 $\pm$ 0.05 pN (averaged over six molecules) and 0.75 $\pm$ 0.04 pN (averaged over four molecules) for short and long handles, respectively. The force jump between the intermediate and unfolded states is equal to 0.66 $\pm$ 0.03 pN (averaged over six molecules) and 0.56 $\pm$ 0.03 pN (averaged over four molecules) for short and long handles, respectively. The shorter force jumps and the faster kinetics observed for the long-handled construct are consistent with their lower effective stiffness (7,8) (see below).

By fitting the transition-rate data using the Bell-Evans theory (Eqs. 1a and 1b) and the detailed-balance condition (Eq. 2), we can obtain the kinetic and thermodynamic parameters characterizing the 3S hairpin (Fig. 5, *A* and *B*, and Table 1). Most of the thermodynamic parameters obtained with short- and long-handled constructs are compatible (see Section S5, Table S5, and Fig. S9). Nevertheless, some differences are observed in the mean free-energy differences and distances between folded, intermediate,

TABLE 1 Kinetic and thermodynamic parameters of the 2S and 3S hairpins

		Bell-Evans						Detailed balance		
	Molecular extension	f^C_{FU}	k^C_{FU}	ΔG_{FU}	$x^{\ddagger}_{FU}$	$x^{\ddagger}_{UF}$	x_{FU}	f^C_{FU}	ΔG_{FU}	x_{FU}
2S SH PM	17.4 ± 0.9	14.8 ± 0.7	1.3 ± 0.2	63.5 ± 1.3	9.3 ± 0.5	8.3 ± 0.4	17.6 ± 0.9	14.8 ± 0.7	63.5 ± 1.4	17.6 ± 0.9
2S SH CFM	18.2 ± 0.9	14.8 ± 0.7	1.5 ± 0.2	73.7 ± 2.7	10.3 ± 0.5	10.1 ± 0.5	20.4 ± 1.0	14.8 ± 0.7	76.9 ± 6.4	21.3 ± 1.8
2S LH PM	17.2 ± 0.9	14.8 ± 0.7	3.8 ± 0.4	66.2 ± 1.2	9.7 ± 0.5	8.7 ± 0.4	18.4 ± 0.9	14.6 ± 0.7	64.5 ± 0.8	18.1 ± 0.9
2S LH CFM	18.2 ± 0.9	14.7 ± 0.7	4.0 ± 0.4	82.9 ± 1.3	12.2 ± 0.6	10.9 ± 0.6	23.1 ± 1.2	14.7 ± 0.7	82.0 ± 1.0	22.9 ± 1.2

		Bell-Evans									
	Molecular extension	f^C_{FI}	f^C_{IU}	k^C_{FI}	k^C_{IU}	ΔG_{FI}	ΔG_{IU}	$x^{\ddagger}_{FI}$	$x^{\ddagger}_{IF}$	$x^{\ddagger}_{IU}$	$x^{\ddagger}_{UI}$
3S SH PM	23.5 ± 1.2	14.6 ± 0.7	12.8 ± 0.6	6.7 ± 0.5	8.8 ± 0.3	50.2 ± 1.2	32.1 ± 1.2	7.4 ± 0.4	6.7 ± 0.3	6.0 ± 0.3	4.4 ± 0.4
3S SH CFM	21.6 ± 1.1	14.3 ± 0.7	13.0 ± 0.6	6.7 ± 0.8	7.6 ± 1.8	56.0 ± 5.1	44.9 ± 3.7	6.4 ± 0.4	9.7 ± 1.7	9.3 ± 0.7	4.9 ± 0.8
3S LH PM	21.0 ± 1.1	14.5 ± 0.7	12.6 ± 0.6	18.1 ± 2.1	11.8 ± 0.6	46.0 ± 1.0	29.5 ± 0.5	8.3 ± 0.4	4.8 ± 0.3	5.6 ± 0.3	4.1 ± 0.2
3S LH CFM	22.5 ± 1.1	14.4 ± 0.7	12.9 ± 0.6	14.6 ± 1.7	9.3 ± 0.6	55.2 ± 4.1	46.0 ± 1.9	9.3 ± 0.8	6.5 ± 0.7	7.4 ± 0.6	7.2 ± 0.4

	Bell-Evans			Detailed balance						
	x_{FI}	x_{IU}	x_{FU}	f^C_{FI}	f^C_{IU}	ΔG_{FI}	ΔG_{IU}	x_{FI}	x_{IU}	x_{FU}
3S SH PM	14.1 ± 0.7	10.3 ± 0.5	24.5 ± 1.2	14.5 ± 0.7	12.9 ± 0.6	52.9 ± 1.4	30.8 ± 0.9	15.0 ± 0.8	9.8 ± 0.5	24.8 ± 1.2
3S SH CFM	16.1 ± 1.6	14.2 ± 1.1	30.3 ± 1.5	14.4 ± 0.7	13.0 ± 0.6	52.2 ± 3.1	43.0 ± 2.7	15.0 ± 0.9	13.6 ± 0.8	28.5 ± 1.4
3S LH PM	13.0 ± 0.7	9.7 ± 0.5	22.7 ± 1.1	14.4 ± 0.7	12.4 ± 0.6	44.9 ± 1.2	27.9 ± 0.5	12.8 ± 0.6	9.2 ± 0.5	22.0 ± 1.1
3S LH CFM	15.7 ± 1.2	14.7 ± 0.7	30.4 ± 1.5	14.4 ± 0.7	12.9 ± 0.6	54.3 ± 3.4	43.6 ± 2.9	15.5 ± 1.0	13.9 ± 1.0	29.4 ± 1.6

Forces are given in pN, transition rates in Hz, energies in k_BT, and molecular extensions in nm. Molecular extensions correspond to values directly extracted from hopping traces. The number of molecules analyzed for each molecular construction was five for 2S SH PM, 2S LH CFM, 3S LH PM, and 3S LH CFM; seven for 2S LH PM, 3S SH PM, and 3S SH CFM; and four for 2S SH CFM. Bell-Evans values were calculated using Eqs. 1a and 1b and detailed-balance values using Eq. 2. Values are represented as the mean ± SE (combination of statistical and instrumental errors) for the different molecules analyzed. We have chosen, as a final estimate of the error, the largest between the two sources of error (statistical and instrumental). 2S, two-state hairpin; 3S, three-state hairpin; SH, short-handled construct; LH, long-handled construct; PM, passive mode; CFM, constant-force mode.

and unfolded states, that lie systematically beyond two error bars. It is interesting that differences in molecular extension between short and long handles are also observed in the values measured for extension jumps in PM traces: 23.5 ± 1.2 nm (averaged over six molecules) and 21.0 ± 1.1 nm (averaged over four molecules) for short and long handles, respectively, showing that the 3S molecule with short handles is thermodynamically more stable than the 3S molecule with long handles. This difference is not negligible (~15%) and might be due to irreversible fraying effects in the stem of the hairpin in the long-handled construct that might be favored by the presence of the longer handles.

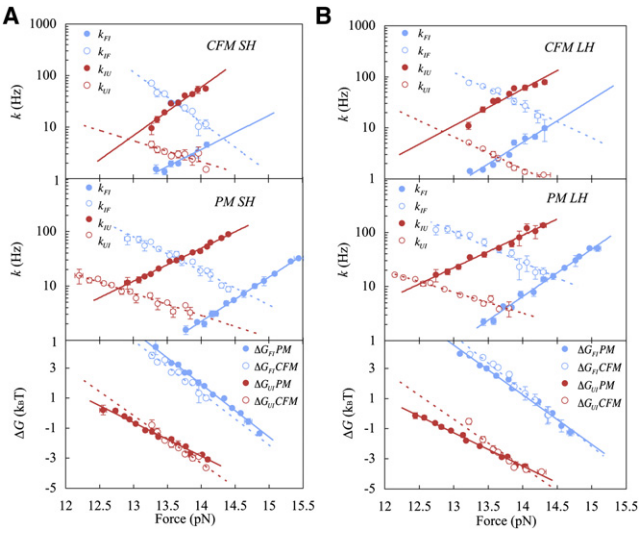

FIGURE 5 Results for the 3S hairpins with short handles (*A*) and long handles (*B*). Plots of k as a function of force for the CFM (*upper*) and PM (*middle*) experiments. Linear fits to the log of the rates are shown, with unfolding rates (k_{FI} and k_{IU}) indicated by solid lines and symbols and folding rates (k_{IF} and k_{UI}) by dotted lines and symbols. (*Lower*) ΔG_{FI} (*blue* or *light gray*) and ΔG_{UI} (*red* or *dark gray*) (color online) versus force for PM (*solid circles*) and CFM (*open circles*). Linear fits are shown as solid lines for PM and dotted lines for CFM. We show the mean values for each point and the to error. Molecule statistics are presented in the note of Table 1.

As previously observed with the 2S hairpin, the transition rates are larger with softer handles: for the long-handled construct, k^C_{FI} and k^C_{IU} are ~2–3 times and 1.25 times larger, respectively, than for the short-handled construct. Note that the kinetics was more affected by handle length in the case of the 2S molecule. This result is consistent with the fact that the 3S molecule presents an intermediate (see below in the Discussion and Conclusions section).

SNR and elastic response of long and short handles

A relevant question in our study is the understanding of how short-handled constructs increase the resolution of our measurements. As explained in the Introduction, one expects a higher SNR for short handles. How much resolution is gained when using short handles as compared to long handles? A careful quantitative evaluation of this question is essential to assess the advantages of the new molecular construct.

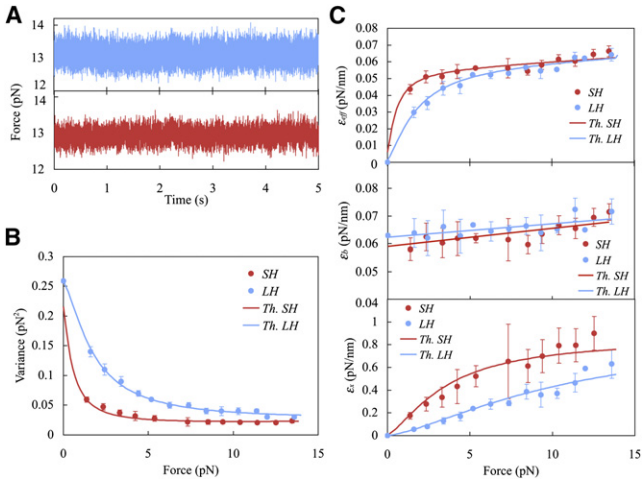

FIGURE 6 Analysis of force variance and stiffness (1–15 pN) for the 2S hairpin. (*A*) Typical force traces (at ≅13 pN) with long (*blue* or *light gray*) and short handles (*red* or *dark gray*) (color online). (*B*) Measured force variance for short (*red* or *dark gray circles*) and long handles (*blue* or *light gray circles*). (*C*) Measured effective stiffness, ε_{eff} (*upper*), stiffness of the trap, ε_b (*middle*), and stiffness of the molecular system, ε_x (*lower*) for short (*red* or *dark gray circles*) and long (*blue* or *light gray circles*) handles. Fits to the elastic model are shown for long (*blue* or *light gray lines*) and short (*red* or *dark gray lines*) handles. Results are the average over three and four different molecules for the short- and long-handle cases, respectively.

SNR with long and short handles

Previous works have shown how the length of the handles, the stiffness of the optical trap, and various instrumental factors influence the measured kinetics of the molecule (2,7,8). The SNR of the measurements, limited by the Brownian motion of the bead $\langle \delta x^2 \rangle$, depends on the stiffness of the molecular construct attached to the bead (handles plus hairpin), ε_x, and that of the trap, ε_b, as given by the fluctuation-dissipation theorem

$$\langle \delta x^2 \rangle = k_B T/(\varepsilon_b + \varepsilon_x) \text{ or } \langle \delta f^2 \rangle = (k_B T \varepsilon_b^2)/(\varepsilon_b + \varepsilon_x), \quad (4)$$

Note that ε_x is the combined stiffness of two serially connected springs, one represented by the handles and the other by the hairpin. Along the folded branch we assume a very rigid hairpin, ε_x being just the stiffness of the handle. According to Eq. 4, the softer (i.e., the longer) the handles, the higher is the noise. When we assume that the jump in extension or force does not depend much on the length of the handles, then, according to Eqs. 3 and 4, the stiffer the linker, the higher is the SNR. To confirm that the SNR is higher with the short-handled construct, we measured the variance of the signal from 1 pN to 15 pN (see Materials and Methods). In Fig. 6 *A*, we show examples of force-time traces for the short- and long-handled constructs and, as shown in Fig. 6 *B*, the force variance is higher with long handles (measured for the 2S hairpin). The SNR measured for the 2S hairpin at the coexistence force is 6.2 ± 0.3 and 8.0 ± 0.8 (averaged over three molecules) for long and short handles, respectively.

To estimate the dependence of the SNR_f on the length of the handles, we proceed as follows. The elastic response of the handle is described by a force-extension relation of the type $f_{L_0}(x) = \widehat{f}(x/L_0)$, where x is the molecular extension and L_0 is the contour length. Then, $\varepsilon_h = (1/L_0) \times (\widehat{f})'(x/L_0)$, meaning that, at a given force f, the stiffness of the handle, ε_h, is inversely proportional to the contour length. The force jump, Δf, between two states at coexistence is given by $\Delta f = \varepsilon_{eff}(f^C_{SS'}) \times \Delta x$, where Δx is the released molecular extension. The effective stiffness, ε_{eff}, of the system is given by

$$1/\varepsilon_{eff}(f) = (1/\varepsilon_b) + (1/\varepsilon_x(f)), \quad (5)$$

where ε_b and ε_x are the rigidities of the trap and the molecular system attached to the bead (handles plus hairpin), respectively. According to Eq. 3 (see Materials and Methods), and using Eq. 4, we find for the SNR the expression

$$SNR_f = \varepsilon_x \Delta x/(k_B T(\varepsilon_x + \varepsilon_b))^{1/2}. \quad (6)$$

In the regime of coexistence forces where $\varepsilon_x >> \varepsilon_b$ we get $SNR_f \cong (\varepsilon_x/k_B T)^{1/2} \Delta x$, showing that, in case $\varepsilon_x = \varepsilon_h \sim 1/L_0$, SNR_f decreases proportionally to the square root of the contour length of the handle. As a consequence, the value of SNR_f for short handles is expected to be five times larger than for long handles. Experimentally we find that the SNR_f is only 1.2 times higher with the short-handled construction, quite far from the expected factor of 5. Therefore, there must be an additional factor that limits the total stiffness of the system ε_x in the short-handled case.

Elastic response of long and short handles

To elucidate where the measured factor 1.2 comes from, we carried out a detailed study of the elasticity of short and long handles from our high-bandwidth measurements. In addition to the force variance shown in Fig. 6 *B*, we also measured the effective stiffness, $\varepsilon_{eff}(f)$, of the molecular setup, defined by $\varepsilon_{eff}(f) = \Delta f/\Delta x$, for the 2S hairpin along the folded branch in a range of forces from 1 pN to the coexistence force, ≅15 pN (Fig. 6 *C*). We measured ε_{eff} over that range of forces by determining the finite derivative, $\Delta f/\Delta x$, along the FDC, where $\Delta f = 1$ pN and Δx is the corresponding trap displacement. The values of the effective rigidities markedly decrease for long handles, especially at low forces. By combining Eqs. 4 and 5, we can solve them at each value of the force and determine the two unknown quantities, ε_b and ε_x, as a function of force from

$$\varepsilon_b = \varepsilon_{eff} + (\langle \delta f^2 \rangle / k_B T), \quad (7)$$

$$\varepsilon_x = ((\varepsilon_{eff} k_B T) + \langle \delta f^2 \rangle)(\varepsilon_{eff}/\langle \delta f^2 \rangle), \quad (8)$$

The results for ε_b and ε_x are shown in Fig. 6 *C*. It is known that the stiffness of an optical trap produced by a Gaussian

beam exhibits nonlinearities at high enough forces (17,18). In Fig. 6 *C* (*middle*), we show the results obtained for the stiffness of the trap and the results of a fit using a linear function of the force. For ε_b, we find $\varepsilon_b = 0.062 + 0.00059f$ (long handles) and $\varepsilon_b = 0.058 + 0.00066f$ (short handles), with ε_b and f expressed in pN/nm and pN units, respectively. Note that in the range of forces explored (1–14 pN), the stiffness of the trap shows a moderate increase from 0.06 to 0.07 pN/nm. The value of the ε_b at zero force is compatible with the trap stiffness measured at high bandwidth (50 kHz) with the bead alone in the trap (no molecule attached) (see Section S6). As shown in Fig. 6 *C* (*lower*), the stiffness of the molecular system differs between the long- and short-handled constructs. Close to the coexistence force (14.5 pN), the stiffness of the short construct is around 1.5 times larger than that in the long-handled construct. Assuming that ε_x gets a contribution from the handles alone (the hairpin is folded), we should expect a factor of 25 (rather than a factor of 1.5) between the two rigidities. Where does this discrepancy come from? We have simultaneously fit the results for $\langle \delta f^2 \rangle$, ε_{eff}, and ε_x by assuming that ε_x is given alone by the elastic response of a handle described by the wormlike chain model with variable persistence length (p) and stretching modulus (Y). Our fits reveal that the persistence lengths of the handles are strongly dependent on their contour lengths: we get $p = 1.6 \pm 0.3$ nm (averaged over three molecules) for the short handles and $p = 31 \pm 3$ nm (averaged over four molecules) for the long handles. These values are markedly lower than the standard value of 45–50 nm reported for half-lambda or lambda DNA (19–24). This decrease of the persistence length has been reported in recent studies of DNA molecules of a few thousand basepairs (25,26) and might be a consequence of the boundary conditions imposed by the fact that the ends of the tethered molecule are anchored to the beads. Indeed, the model proposed in Seol et al. (25) predicts persistence lengths between 20 and 30 nm for DNA molecules of 500–800 bp (close to the size of long handles) attached between two beads, values that are not far from our measurement of persistence length for long handles ($\cong$30 nm). For the stretching modulus we find $Y = 390 \pm 40$ pN (averaged over four molecules) for long handles and $Y = 16.9 \pm 1.3$ pN (averaged over three molecules) for short handles, showing a concomitant marked decrease of the enthalpic elasticity for very short DNA molecules (see Section S8 for details of the stretching modulus).

DISCUSSION AND CONCLUSIONS

In this work, we introduced what to our knowledge is a new minimal construct for single-molecule manipulation with very short (29-bp) handles. We investigated two different DNA hairpin structures using the new short-handled construct and compared the results with those obtained with conventional constructs (~700-bp handles). One hairpin was designed to behave as an ideal two-state folder (2S hairpin), whereas the other has a fast intermediate-state on-pathway (3S hairpin). To investigate the folding/unfolding kinetics of these hairpins, we carried out hopping experiments in PM and CFM (7,8,12). As a general trend, the thermodynamic parameters (coexistence forces, molecular extensions, and folding free energies) obtained from the analysis of the hopping traces for the two different constructs yield consistent results for both the 2S and 3S hairpins (see Tables 1 and 2 and Figs. 4 and 5). However, we found that the 3S hairpin in the long-handled construct is found to be 15% shorter and less thermodynamically stable than in the short-handled construct. We speculate whether the long handles induce a residual but permanent fraying at the stem of the 3S hairpin. As expected, the main differences between the two constructs appear when comparing the folding/unfolding rates: the higher effective stiffness of the experimental setup in the new minimal construct leads to slower kinetics (7,8,2). Note that the noise in the force and extension traces decreases when using the short handles, leading to a higher SNR (7,8,13). Therefore, using stiff handles might be desirable to increase not only the spatial or force resolution (SNR) but also the time resolution by slowing down fast structural transitions that otherwise might not be detected.

Why are the coexistence rates higher for long handles compared to short handles? The explanation is the basepair hopping effect discussed in Manosas et al. (8): during the short timescale at which individual basepairs along the hairpin breathe, the bead in the trap does not respond, and as a consequence, the force acting on the basepair changes (it increases if the basepair forms and decreases if the basepair dissociates), slowing the overall folding-unfolding kinetics. This change in force is lower for long handles compared to short handles, making the overall kinetics faster in the former case. In addition, for the 2S hairpin, the coexistence rate for the long-handled construct is 3–4 times that for the short-handled construct. For the 3S hairpin, this factor is smaller,2–3 times for the coexistence rate between the folded and intermediate states and 1.25 times between the intermediate and unfolded states. The magnitude of such a factor appears to correlate with the released molecular extension. Indeed, the larger molecular extension released by the 2S hairpin for the F-U transition ($\cong$18 nm) should be compared to the shorter extension for the F-I ($\cong$12 nm) and I-U ($\cong$10 nm) transitions in the 3S hairpin. This leads to a bigger difference in the overall folding-unfolding kinetics between short and long handles for the 2S hairpin.

If the handles are too short, might the beads interact with each other and distort the measurements? Not with the current setup. The mean excursion of a trapped bead is given by the equipartition relation, $x_{\mathrm{RMS}} = \sqrt{k_{\mathrm{B}}T/(\varepsilon_b + \varepsilon_x)}$. At 15 pN, the rigidity of the DNA tether is much larger than that of the trap, $\varepsilon_x >> \varepsilon_b$. If we take $\varepsilon_x \cong 1$ pN/nm

(see Fig. 6 *C*, *lower*), we get $x_{RMS} \approx 2$nm, which is 10 times smaller than the expected contour length of 2×29 bp, which is ~20nm. No clashing between the beads is then expected or observed under such conditions. On the other hand, we cannot exclude the possibility that the hairpin under a tension does not interact with the beads. This effect should be important only when the length of the hairpin is larger than the length of the handles and fluctuations of the hairpin axis along the stem are big enough for the hairpin to align along the pulling direction. Our experiments show that this effect is small, though.

Another remarkable result in this study concerns the elastic properties of long and short handles. It is interesting to note that the SNR for short handles is found to be only 1.2 times the value for long handles, when we originally expected a factor of 5. How is that possible given the fact that the short handles, being 25 times shorter than long handles, are expected to be ~25 times more rigid? The answer lies in the measured elastic response of short and long DNA molecules tethered between two beads. The strong decrease observed in the persistence length and stretching modulus of the dsDNA handles when their contour length is reduced from $\cong 700$ bp to 29 bp contributes to the drastically attenuate increase in stiffness. A moderate decrease in the persistence length of dsDNA molecules (a few kb long) when tethered between two beads has been already reported (25,26). However, within the present range of much shorter molecules (between 20 bp and 700 bp), these effects seem to strongly increase. According to the extensible wormlike chain model, the compliance of a dsDNA molecule at high forces behaves like $1/\varepsilon_x = [L_0/(4p/k_BT)^{1/2}]f^{-3/2} + L_0/Y$, where the first and second terms are the entropic and enthalpic contributions, respectively (see Section S8). For the long handles pulled at forces $\cong 15$ pN, the sum in $1/\varepsilon_x$ is dominated by the entropic elasticity term, whereas for the short handles, with a strong decrease in the stretching modulus, the biggest contributor to overall compliance is the enthalpy term. Our experimental results show that the marked decrease in persistence length and stretching modulus of the short DNA tethers strongly limits the value of the stiffness, ε_x, of the whole molecular setup, establishing an upper bound ($\varepsilon_x \cong 1$ pN/nm) to the maximum value that we can achieve for the SNR. The observed strong decrease of the stretching modulus for the short DNA handles is suggestive of a failure of the elastic rod model applied to short DNA molecules, a result that has been recently reported from small-angle x-ray scattering measurements (27) and that should be corroborated in future mechanical experiments. However, another explanation is possible (28,29). In addition to the boundary effects considered in Seol et al. (25), at least three effects might contribute to decrease the overall stiffness of the handles (resulting in underestimated values of the persistence length and stretch modulus). First, in the process of labeling one of the handles with digoxigenins, a terminal transferase reaction is used to generate a dig-labeled ssDNA flexible tail. The length of such a tail will influence the effective stiffness of the tether. Second, nonspecific interactions between handles and bead could also induce irreversible fraying of the handles, resulting in additional single-stranded ends. Finally, the biotin/streptavidin and dig/antidig bonds might contribute with an additional soft component as well. Although we do not know which effect among these is the dominant one, all of them conspire to reduce the overall stiffness of the linker. This is in agreement with what we observe.

Summing up, we have introduced what to our knowledge is a new methodology of synthesizing molecular constructs with short handles that has several advantages. First, the synthesis of the new molecular construct is easier to implement compared to the long-handled synthesis. Second, this new minimal construct can be used to moderately enhance the SNR of the measurement. Third, the kinetics of the short-handled construct is slower, allowing us to measure fast hopping transitions that might not be detected with conventional longer constructs. Finally, we have presented what we believe is a novel method to extract accurate information about the elastic properties of the molecular setup based on high-bandwidth measurements of force fluctuations. This method of analysis has two main applications: it can be used to determine the stiffness of the trap and, at the same time, can be used to extract accurate information about the elastic properties of generic polymers. This methodology could be extended to other types of handles and systems such as RNAs and proteins that exhibit more complex molecular folding landscapes.

SUPPORTING MATERIAL

Eight sections, a table, figures, and references are available at http://www.biophysj.org/biophysj/supplemental/S0006-3495(11)00201-3.

M.M. is supported by the Human Frontier Science Program (RGP0003/2007-C) and the European Union BioNanoSwitch. K.H. is supported by the JSPS fellowship (No. 193179). J.M.H. is supported by the Spanish Research Council in Spain. F.R. is supported by grants from the Spanish Research Council (FIS2007-3454), the Institució Catalana de Recerca i Estudis Avançats Academia Awards 2008, and the Human Frontier Science Program (RGP55-2008).

REFERENCES

1. Ritort, F. 2006. Single-molecule experiments in biological physics: methods and applications. *J. Phys. Condens. Matter.* 18:531–583.
2. Greenleaf, W. J., M. T. Woodside, …, S. M. Block. 2005. Passive all-optical force clamp for high-resolution laser trapping. *Phys. Rev. Lett.* 95:208102.
3. Liphardt, J., B. Onoa, …, C. Bustamante. 2001. Reversible unfolding of single RNA molecules by mechanical force. *Science.* 292:733–737.
4. Woodside, M. T., W. M. Behnke-Parks, …, S. M. Block. 2006. Nanomechanical measurements of the sequence-dependent folding landscapes of single nucleic acid hairpins. *Proc. Natl. Acad. Sci. USA.* 103:6190–6195.

5. Woodside, M. T., P. C. Anthony, …, S. M. Block. 2006. Direct measurement of the full, sequence-dependent folding landscape of a nucleic acid. *Science.* 314:1001–1004.

6. Mossa, A., M. Manosas, …, F. Ritort. 2009. Dynamic force spectroscopy of DNA hairpins: I. Force kinetics and free energy landscapes. *J. Stat. Mech.* 2009:P02060.

7. Wen, J.-D., M. Manosas, …, I. Tinoco, Jr. 2007. Force unfolding kinetics of RNA using optical tweezers. I. Effects of experimental variables on measured results. *Biophys. J.* 92:2996–3009.

8. Manosas, M., J.-D. Wen, …, F. Ritort. 2007. Force unfolding kinetics of RNA using optical tweezers. II. Modeling experiments. *Biophys. J.* 92:3010–3021.

9. Katz, E., and I. Willner. 2004. Biomolecule-functionalized carbon nanotubes: applications in nanobioelectronics. *ChemPhysChem.* 5:1084–1104.

10. Yokokawa, R., J. Miwa, …, M. Kasahara. 2008. DNA molecule manipulation by motor proteins for analysis at the single-molecule level. *Anal. Bioanal. Chem.* 391:2735–2743.

11. Huguet, J. M., C. V. Bizarro, …, F. Ritort. 2010. Single-molecule derivation of salt dependent base-pair free energies in DNA. *Proc. Natl. Acad. Sci. USA.* 107:15431–15436.

12. Li, P. T. X., D. Collin, …, I. Tinoco, Jr. 2006. Probing the mechanical folding kinetics of TAR RNA by hopping, force-jump, and force-ramp methods. *Biophys. J.* 90:250–260.

13. Hyeon, C., G. Morrison, and D. Thirumalai. 2008. Force-dependent hopping rates of RNA hairpins can be estimated from accurate measurement of the folding landscapes. *Proc. Natl. Acad. Sci. USA.* 105:9604–9609.

14. SantaLucia, Jr., J. 1998. A unified view of polymer, dumbbell, and oligonucleotide DNA nearest-neighbor thermodynamics. *Proc. Natl. Acad. Sci. USA.* 95:1460–1465.

15. Zuker, M. 2003. Mfold web server for nucleic acid folding and hybridization prediction. *Nucleic Acids Res.* 31:3406–3415.

16. Onoa, B., S. Dumont, …, C. Bustamante. 2003. Identifying kinetic barriers to mechanical unfolding of the *T. thermophila* ribozyme. *Science.* 299:1892–1895.

17. Ashkin, A. 1992. Forces of a single-beam gradient laser trap on a dielectric sphere in the ray optics regime. *Biophys. J.* 61:569–582.

18. Simmons, R. M., J. T. Finer, …, J. A. Spudich. 1996. Quantitative measurements of force and displacement using an optical trap. *Biophys. J.* 70:1813–1822.

19. Hagerman, P. J. 1988. Flexibility of DNA. *Annu. Rev. Biophys. Biophys. Chem.* 17:265–286.

20. Fixman, M., and J. Kovac. 1973. Polymer conformational statistics. III. Modified Gaussian models of stiff chains. *J. Chem. Phys.* 58:1564–1568.

21. Bustamante, C., J. F. Marko, …, S. Smith. 1994. Entropic elasticity of λ-phage DNA. *Science.* 265:1599–1600.

22. Marko, J. F., and E. D. Siggia. 1995. Stretching DNA. *Macromolecules.* 28:8759–8770.

23. Wang, M. D., H. Yin, …, S. M. Block. 1997. Stretching DNA with optical tweezers. *Biophys. J.* 72:1335–1346.

24. Bouchiat, C., M. D. Wang, …, V. Croquette. 1999. Estimating the persistence length of a worm-like chain molecule from force-extension measurements. *Biophys. J.* 76:409–413.

25. Seol, Y., J. Li, …, M. D. Betterton. 2007. Elasticity of short DNA molecules: theory and experiment for contour lengths of 0.6–7 microm. *Biophys. J.* 93:4360–4373.

26. Chen, Y.-F., D. P. Wilson, …, J. C. Meiners. 2009. Entropic boundary effects on the elasticity of short DNA molecules. *Phys. Rev. E.* 80:020903.

27. Mathew-Fenn, R. S., R. Das, and P. A. B. Harbury. 2008. Remeasuring the double helix. *Science.* 322:446–449.

28. Becker, N. B., and R. Everaers. 2009. Comment on "Remeasuring the double helix". *Science.* 325:538b.

29. Mathew-Fenn, R. S., R. Das, …, P. A. B. Harbury. 2009. Response to comment on "Remeasuring the double helix". *Science.* 325:538c.